



Changes in tidal asymmetry in the German Wadden Sea

Robert Hagen¹ · Christian Winter² · Frank Kösters¹

Received: 13 September 2021 / Accepted: 25 March 2022 / Published online: 12 April 2022
© The Author(s) 2022

Abstract

The recent morphological development of the German Wadden Sea (North Sea, Europe) has been characterized by expanding intertidal flats and deepening, narrowing tidal channels at declining subtidal volume. This study analyzes the effect of these changes on tidal asymmetry, based on numerical modeling with high-resolution bathymetry data, and discusses possible adaptations of the import and export behavior in intertidal systems. As common descriptors of tidal asymmetry may show a high spatial variability in bathymetrically complex intertidal systems, we develop a novel subregion averaging approach for a more robust trend estimation. Our data reveal a statistically significant decrease in flood and flood current duration in the period from 1996 to 2016 resulting in declining flood dominance or enhanced ebb dominance in most tidal basins of the German Wadden Sea. Mean and peak current asymmetry also indicate significant decreases in mean flood current magnitude. We relate decreasing flood dominance mostly to local bathymetric volume changes rather than tidal amplitude. However, it appears likely that the sum of local effects facilitates the adaptation of regional tidal dynamics which affects especially the northern German Bight. This regional shift is explained by the deceleration of rising tides due to increased friction on laterally expanded intertidal flats and decreased subtidal channel volume. The decrease in flood or increase in ebb dominance, respectively, indicates that the recent trend of sediment accretion in Wadden Sea areas may cease soon.

Keywords North Sea · Wadden Sea · Tides · Tidal asymmetry · Tidal channels · Sea level rise · Morphodynamics

1 Introduction

The Wadden Sea is the largest coherent intertidal flat area worldwide and a UNESCO world heritage site. This precious ecosystem spans the Dutch, German, and Danish North Sea coast with a distinct richness of terrain forms, e.g., extensive open and back-barrier intertidal flats, branched tidal channels, sandbanks, and barrier islands. External dynamics such as sea level rise (Idier et al. 2017), spatially varying changes in tidal range (Jänicke et al. 2020), nonlinear tide-tide interactions on shorter (Gräwe et al. 2014; Müller et al. 2014), and longer time scales (Hagen et al. 2021a) constantly alter hydro- and morphodynamics in this area. A recent analysis of the German Wadden Sea bathymetry has revealed a lateral and vertical expansion of intertidal flats along with a deepening of

tidal channels at decreasing subtidal channel volume. In other words, intertidal areas are expanding, and narrower, deeper tidal channels are prevailing (Benninghoff and Winter 2019).

Drivers and effects, i.e., the interaction between observed bathymetry changes and tidal dynamics, remain unclear at this point. Analytical solutions and 1D modeling suggest a link between basin hypsometry (Friedrichs 2011), tidal flat geometry (Pritchard and Hogg 2003), intertidal storage volume (Friedrichs and Aubrey 1988), and tidal asymmetry. Tidal asymmetry can be described as the ratio of flood and ebb characteristic values for sea surface elevation and current velocity over a tidal cycle. Shorter flood duration is connected to flood dominance, as it is associated with stronger flood current velocity and increased sediment transport potential. In practice, a direct estimation of flood and ebb dominance, e.g., by current observations, is hampered by a lack of reliable measurements. Other approaches therefore describe the asymmetry of a tidal signal by phase ratios (e.g., the 2M2-M4 phase lag) of tidal constituents (Friedrichs and Aubrey 1988; Song et al. 2011). Flood or ebb dominance in an estuary can also be estimated by geometrical relationships such as the ratio between tidal amplitude and mean

✉ Robert Hagen
robert.hagen@baw.de

¹ Federal Waterways Engineering and Research Institute, BAW, Hamburg, Germany

² Institute of Geosciences, Christian-Albrechts-Universität Zu Kiel, CAU, Kiel, Germany

channel depth (a/h), volume considerations, or intertidal width changes within a tidal cycle (Friedrichs and Aubrey 1988; Friedrichs and Madsen 1992).

To understand the hydrodynamic changes in the context of recent bathymetry evolution in the German Wadden Sea area, we investigate the development of tidal asymmetry by dedicated numerical modeling of annual morphological states. Previous studies on the possible consequences of near-coast bathymetry changes for tidal dynamics were based on model simulations of the years 2000 and 2011. They showed a local and regional impact on 2M2-M4 phase lag in North Frisia and the German estuaries (Jacob et al. 2016). The applicability of the 2M2-M4 parameter, however, is disputable in the southern German Bight, as, e.g., M4 amplitudes are locally more than 50 times smaller than M2. Another study investigating sea level rise in the German Bight showed that the changes in peak current velocity asymmetry are negligible if intertidal flats are elevated and channels are deepened accordingly (Wachler et al. 2020). However, this effect was solely investigated by applying a uniform increase in the intertidal flats' height, instead of varying their elevation and lateral extent, which can be expected based on Benninghoff and Winter's (2019) observations. Recently, a conceptual morphodynamic model of a tidal basin has shown that sea level rise enhances the lateral expansion of tidal flats and increases sediment export (Guo et al. 2021). Another modeling approach investigated the effect of (again uniform) vertical intertidal flat accretion in combination with sea level rise scenarios and concluded that the M2 amplitude as well as the 2M2-M4 phase lag will adapt to the changes if the intertidal areas cannot keep up with sea level rise (Jordan et al. 2021). Other numerical studies of large-scale sea level rise scenarios in the Wadden Sea either neglect the effect of nearshore bathymetry (Pickering et al. 2012), they focus on isolated tidal basins (Becherer et al. 2018; Hofstede et al. 2018), or lack detailed grid resolution in the Wadden Sea (Idier et al. 2017; Pickering et al. 2017).

This study uses numerical modeling data (Hagen et al. 2021b) which are based on the most recent available data on the morphological development in the German Wadden Sea to reveal changes in tidal asymmetry. Our goal is the quantification of changes in sea surface elevation and current velocity asymmetry as an estimator for changes in the sediment import and export behavior of tidal subsystems in the German Wadden Sea. We focus on tidal channels as the main pathways of sediments on long time scales and utilize annual harmonic constituents and tidal characteristic values in the period from 1996 to 2016 to derive trends of tidal characteristic values and tidal asymmetry. Thus, our study aims to provide a foundation for potential driving mechanisms to understand the relationship between bathymetry, regional tidal dynamics, and local tidal asymmetry changes.

This paper is structured as follows: In Sect. 2, we define the evaluated tidal asymmetry parameters used throughout this paper and our analysis methodology. In Sect. 3, we first aim to establish whether our model data can reproduce tidal asymmetry before investigating the mechanisms behind changing tidal asymmetry. To this end, we need to assess the changes in tidal characteristic parameters and current velocity. Section 3 concludes by analyzing trends in flood to ebb ratios and deriving the changes in mean flood and mean ebb current velocities. Section 4 focuses on a discussion of the potential causes of shifts in tidal asymmetry.

2 Methods

2.1 Tidal asymmetry

Different descriptors may be used to quantify tidal asymmetry. The amplitude ratio between shallow water and main tidal constituents (e.g., the M4 to M2 amplitude ratio) is an indicator of asymmetry strength, and the phase lag (e.g., the 2M2-M4 phase lag) can estimate if flood- or ebb dominance is present (Friedrichs and Aubrey 1988). Alternatively, tidal characteristic value ratios such as flood to ebb duration describe asymmetry strength and dominance simultaneously for each tide, including episodic disturbance from, e.g., storm surges. The duration asymmetry of flood and ebb has been mentioned as an indicator of the residual transport of fine suspended sediments, while velocity asymmetry may be used to estimate the transport of coarser suspended material (Dronkers 1986; Friedrichs and Aubrey 1988). Flood and ebb (mean and peak) current velocities were also found to be dominant for sand transport in 1D modeling (van Maren and Winterwerp 2013; Zhou et al. 2015). For this reason, we have chosen the 2M2-M4 phase lag, as well as the duration and velocity asymmetry descriptors in Table 1 following Dronkers' (1986) ideas. The parameters from Table 1 are illustrated graphically in Fig. 1.

It should be noted that we use flood to tide duration ratio instead of the flood to ebb duration ratio to avoid a nonlinear amplification of flood dominance. If, for example, flood duration decreases from 400 to 300 min along a tidal cycle of 700 min, the flood to ebb duration ratio changes nonlinearly from 1.33 to 0.75 and the flood to tide duration ratio changes linearly from 0.57 to 0.43.

Moreover, geometrical relationships such as the ratio a/h between the mean tidal amplitude a (here: half of the annually averaged tidal range within tidal channels) and the mean subtidal channel depth h and the ratio between the intertidal storage volume V_s and the subtidal channel volume V_c (Friedrichs and Aubrey 1988) are applied to estimate the tidal asymmetry of short, shallow estuaries (i.e., tidal channels). V_s is hereby defined as the intertidal storage volume at high water, and V_c is defined as the subtidal channel volume at

Table 1 Overview of applied tidal asymmetry parameters

Tidal asymmetry parameter	Flood dominance	Symmetry	Ebb dominance
2M2-M4 phase lag (sea surface)	0–180°	180, 360°	180–360°
Flood (T _F) to tide (T _T) duration	< 0.5	0.5	> 0.5
Flood (T _f) to tide (T _t) current duration	< 0.5	0.5	> 0.5
Mean flood ($v_{f,mean}$)-to-mean ebb ($v_{e,mean}$) current velocity magnitude ratio	> 1	1	< 1
Peak flood ($v_{f,peak}$)-to-peak ebb ($v_{e,peak}$) current velocity magnitude ratio	> 1	1	< 1

mean water (Friedrichs 2010). Although local flood and ebb dominance depends on the presence of intertidal storage volume, a numerical solution provided by Friedrichs and Aubrey (1988) has established that small ah ratios favor ebb dominance (assuming the presence of intertidal storage volume), while larger values indicate flood dominance. If no intertidal storage volume is present, a system tends to be flood dominant, independently of the ah ratio.

An increase in ah therefore indicates either an increase in tidal range or a decrease in mean channel depth and is associated with flood dominance. An increase in V_s/V_c enhances ebb dominance at small ah and would result from a lateral expansion of intertidal flats, changing mean tidal flat height, or decreasing mean channel depth or width.

2.2 Data availability and analysis

Numerical modeling results for sea surface elevation, tidal constituents, tidal characteristic values, and bathymetry data were acquired from the EasyGSH-DB data collection (Hagen et al. 2020; Sievers et al. 2020). The data collection contains hindcasts of tidal dynamics in the German Bight for the period from 1996 to 2015. Using the same modeling system, we added the year 2016 to these data to obtain a larger number of samples for trend estimation. Details of the 3D numerical model including model setup and validation are described in Hagen et al. (2021b) and the model domain is illustrated in Fig. 2.

Tidal constituents and tidal characteristic values in the EasyGSH-DB data were computed from annual numerical simulations and processed from 10-min intervals to approximately 705 tidal cycles for each year. Afterward, annual means of tidal characteristic values were calculated with each flood and ebb tidal characteristic value weighted by tide duration. We used annual harmonic analysis and annually averaged tidal characteristic values intentionally, as the spring-neap variation induces a high amount of variability, which hampers statistically significant trend estimation on longer time scales. Accordingly, we assumed interannual variation and meteorological oscillation to even out through averaging, although we understand that this may impose a limitation on our results.

It should be noted that our current velocity analysis method requires a bidirectional flow with a main flow direction to be able to distinguish between flood and ebb current. For this reason, tidal events in a multidirectional flow situation, e.g., near amphidromes with low tidal range or close to strong wave-current interaction, were excluded from subsequent analysis. Data affected by intertidal wetting and drying were also dismissed. Excluded values are referred to as invalid in the following.

2.3 Morphological unit averaging approach

Tidal asymmetry is a function of depth changes, channel convergence, tidal range, and intertidal width changes (Friedrichs 2010). Dissipation of tidal energy in shallow

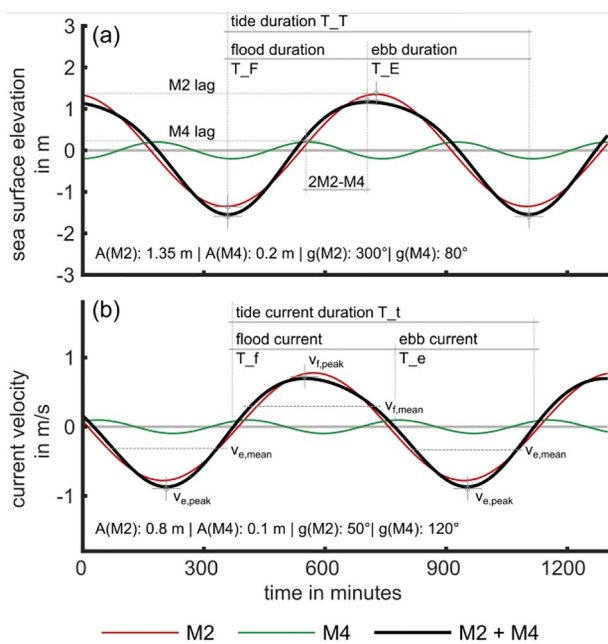


Fig. 1 Schematic flood dominant tidal cycle (black line) from the tidal constituents M2 (red line) and M4 (green line) at the tidal gauge KNO (see Fig. 3). The tidal asymmetry descriptors from Table 1 are indicated for sea surface elevation (a) and current velocity (b)

water leads to the generation of overtides, which causes flood or ebb dominance. In complex bathymetric environments, shifts of flood vs. ebb dominance can happen on small spatial scales within hundreds of meters. For this reason, we conducted spatial averaging of tidal asymmetry values over small subareas, which allowed us to obtain robust results for spatially variable tidal asymmetry descriptors in defined morphological subsystems (i.e., morphological units). The spatial mean of a tidal asymmetry descriptor was subsequently taken as representative of a morphological unit instead of individual tide gauge locations. These morphological unit averages were applied in our trend analysis.

In this paper, we defined morphological units (see Fig. 3 and supplement D) for each tidal basin, via estuarine geometry or near the location of a tide gauge. A morphological unit must cover the tidal channels of interest within the entire analysis period. Therefore, some supratidal and intertidal areas close to the coastline are excluded as well as areas with artificial morphological changes by, e.g., port construction or dredging. We limited shoreface polygons (e.g., 11, 15, 20) seawards roughly by the -15 mNHN isobath (with NHN being German chart datum), and inlet polygons (e.g., 5 to 9) include a small portion of the channel delta up to approximately the -20 mNHN isobath. Additionally, the outer estuaries of the rivers Ems (1 to 4), Jade (11 to 14), Weser (15

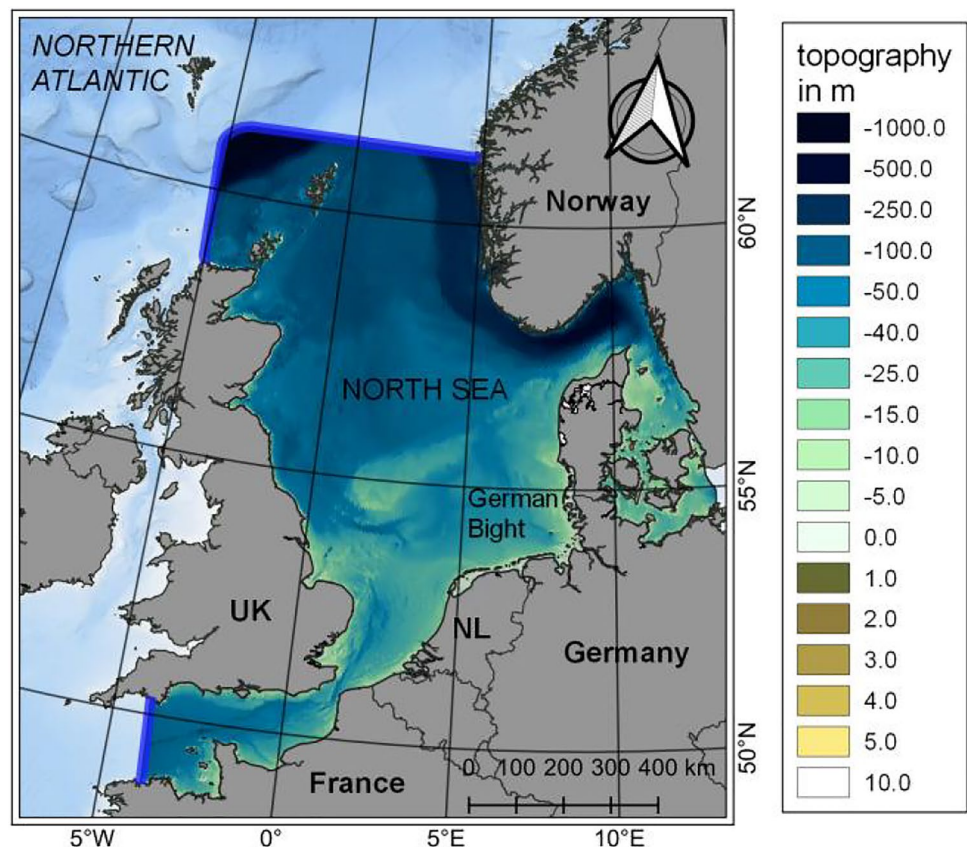
to 19) and Elbe (20 to 25) were divided into multiple units which mainly depend on the location of tide gauges (e.g., green triangles in Fig. 3).

As an example, Fig. 4(a) demonstrates the spatial variability for the annually averaged peak flood to peak ebb current velocity magnitude ratio in the inner Jade Bay (morphological unit 13 in Fig. 3). Starting from a full spatial coverage (see Fig. 4(a)), data with invalid tidal events (see Sect. 2.2) were excluded (Fig. 4(b)) and clipped to a chosen morphological unit area (Fig. 4(c)) before being averaged within the unit (Fig. 4(d)). We can only consider samples in permanently inundated areas with a predominantly bidirectional flow in the following (i.e., tidal channels) because information about a full tidal cycle is required. As our original data are distributed on unstructured grids, averaging was carried out considering the unstructured elements area.

2.4 Trend analysis

We carried out a linear regression analysis on annually averaged parameters in each morphological unit (e.g., data from Fig. 4(d), referred to as “samples” below) for the period from 1996 to 2016. The good agreement in our fitting results suggested that linear regression is suitable for the chosen period.

Fig. 2 The EasyGSH-DB data collection modeling domain (adapted from Hagen et al. 2021b) illustrating open boundaries (solid blue lines) and model topography



It should be noted that this may not be the case on longer time scales with non-linear behavior due to an accelerated sea level rise and long-term tidal cycles such as the nodal tide. Furthermore, we tested linear regression results for statistical significance (significance hereafter) by performing an *F*-test at a 5% significance level and established an outlier check to improve regression robustness. We rejected samples which depart more than three scaled, median, and absolute deviations from the sample median in trend analysis. An outlier check became inevitable because of implausible height jumps in the bathymetry before airborne laser scanning technology was available, which resulted in obvious local outliers even within morphological averages.

3 Results

3.1 Tidal asymmetry at gauges and morphological units

We aggregated large quantities of data in each morphological unit using the morphological unit averaging approach (MUA; see Sect. 2.3). For this reason, we first need to establish whether the model can reproduce tidal asymmetry sufficiently by comparing observed and predicted tidal

asymmetry descriptors at tide gauges (see Table 2). In addition, we evaluated how morphological averages correspond to measured and modeled data at gauges. This specific comparison of modeling results and observations contributes to the numerical model validation given in Hagen et al. (2021b). We selected several tide gauges in the study area to cover different morphological conditions (see Fig. 3) including estuarine (e.g., KNO or BAL), tidal inlet (e.g., NOY, SPI), or outer estuary tidal channels (e.g., ALW, CUX). We conducted a comparison for sea surface asymmetry only, as the spatial coverage and survey quality of available current velocity measurements were insufficient in the study area.

Observed M2 amplitudes range from 0.97 m in HOH to 1.77 m in WAV. The M4/M2 amplitude ratio rarely exceeds 0.08 within the entire study area for observation, prediction, and morphological averages alike. Measured minimum M4/M2 amplitude ratios range from 0.02 in NOY and SPI to 0.13 in KNO, with a maximum deviation between observation and prediction of 0.03 at BAL. Predicted and morphologically averaged values agree at most locations, although notable differences exist in NOY and BUS. The 2M2-M4 phase lag shows more pronounced differences between observed and predicted values with more than 30° in NOY, SPI, and WAV to less than 10° at other gauges. 2M2-M4 further deviates by several degrees between the predicted gauge value and

Fig. 3 Topography of the study area (bottom, right) and location within the North Sea (top left). Morphological units are indicated by black solid lines and a unit ID (1 to 32). Tide gauge stations are represented by green triangles with a three-letter code

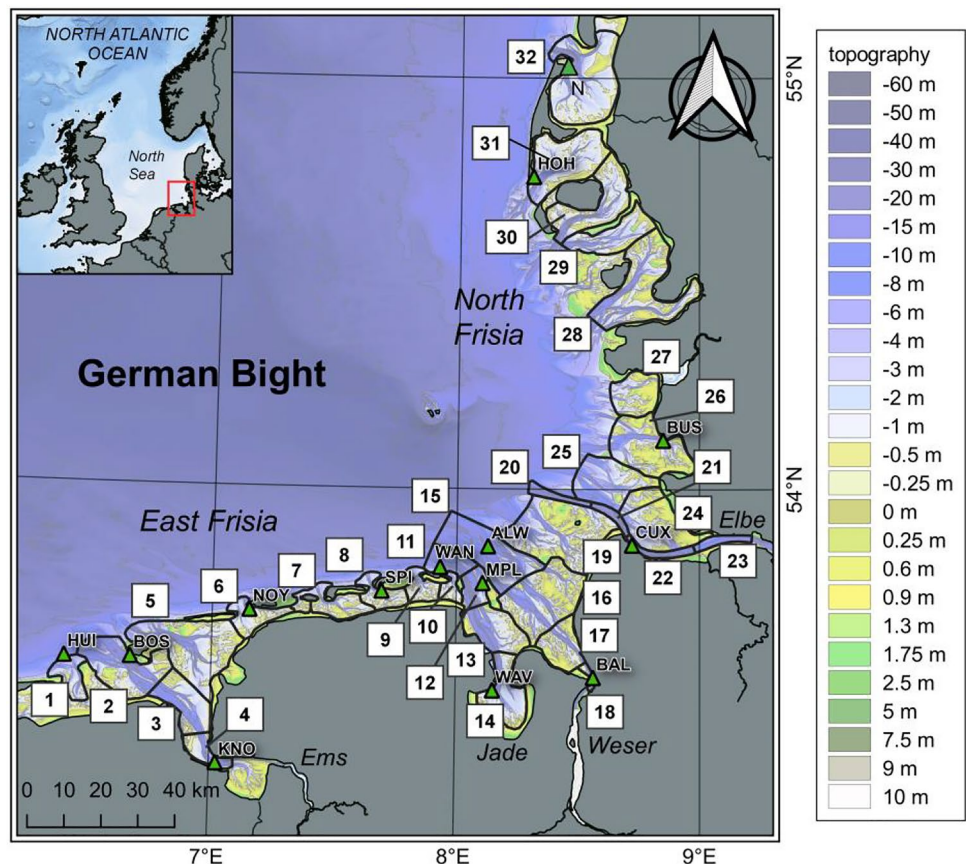
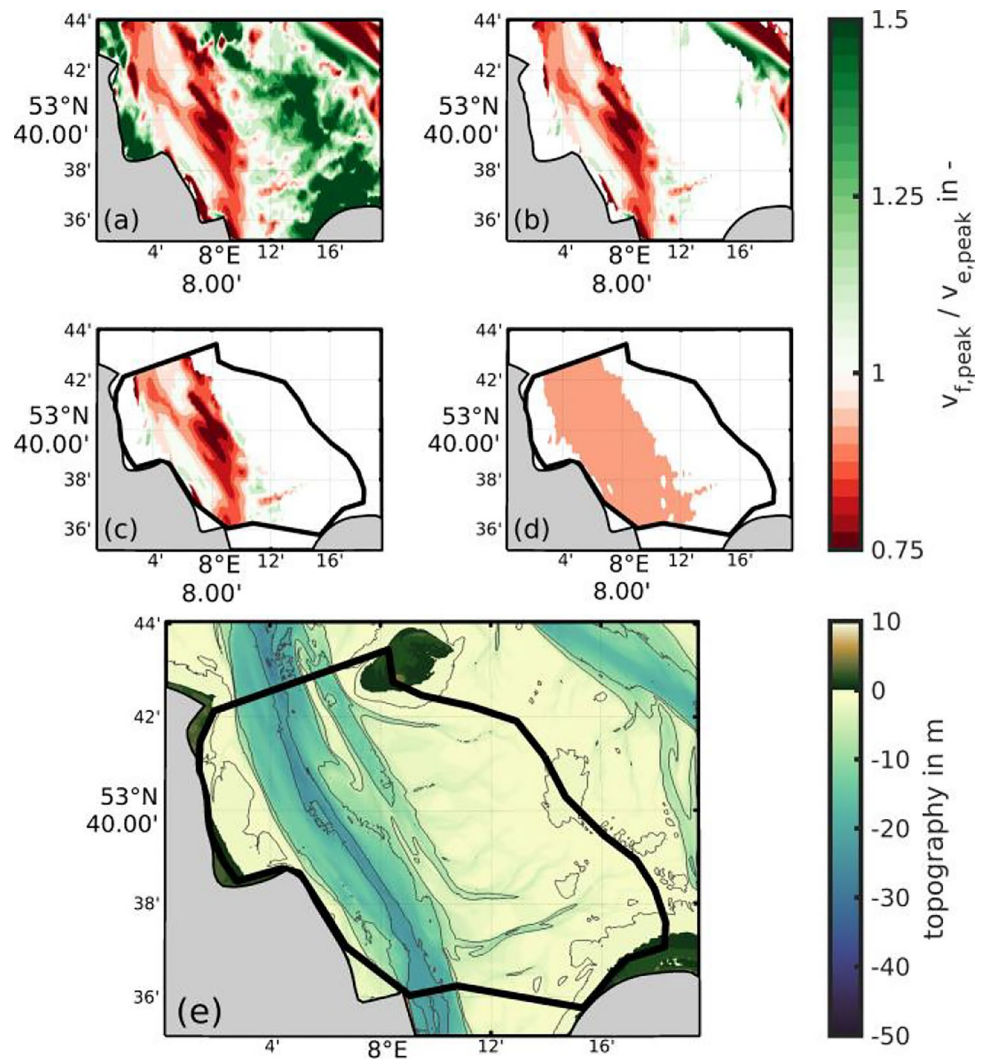


Fig. 4 Calculation of the morphological average of the mean peak flood to peak ebb current velocity ratio in unit 13 (see Fig. 3) in the year 2015. Red values indicate ebb dominance; green values indicate flood dominance. First, data points with invalid tidal events were excluded (b) from the analyzed data. Second, data outside the morphological unit were clipped (c) before being averaged within the morphological unit (d). Panel (e) shows the topography of unit 13 (black lines), and the -40 -, -30 -, -20 -, -10 -, -5 -, and 0 -mNHN isobaths (gray lines)



the morphological averages; the agreement with the measurements is in some cases better (e.g., WAV, CUX) and in other cases poorer (e.g., NOY, BAL). We observe that large differences of 2M2-M4 phase lags between observation, prediction, and morphological average coincide with low M4/M2 ratios. Additionally, the predicted 2M2-M4 phase lag indicates that the model often suggests stronger flood dominance than corresponding observations.

The flood to tide duration ratio (T_F/T_T) compares well between observation, prediction, and morphological averages with maximum gauge prediction differences of 0.03 in HOH. Nonetheless, most differences between observation and prediction or morphological average are below 0.01, with morphological averages indicating a better overall fit to observations.

In summary, our results show that low M4/M2 amplitude ratios coincide with larger differences between observed and predicted or morphologically averaged 2M2-M4 phase lags, while T_F/T_T remains robust even at low M4/M2 ratios for gauge prediction and morphological average. 2M2-M4 phase

lag and T_F/T_T both indicate similar flood or ebb dominance whenever the M4/M2 amplitude ratio is larger than 0.07. Reasonable agreement between modeled and measured T_F/T_T ratios has led us to presume that the model can reproduce representative tidal asymmetry in the study area. Nevertheless, differences of 2M2-M4 phase lags at low and medium M4/M2 amplitude ratios and gauge prediction deviations of the T_F/T_T comparisons in BUS and HOH show that analysis results at tide gauges are susceptible to local effects. Considering the spatially variable distribution of the peak current velocity in Fig. 4(a), point data may not be suitable for the estimation of long-term trends in current velocity asymmetry because of bathymetry sensitivity.

3.2 Local and regional changes in flood duration

To obtain an overall impression of changes in tidal asymmetry, the difference between the annually averaged flood duration in 1997 and in 2015 was calculated in Fig. 5. Both

Table 2 Annual average of M2 amplitude A (M2) and comparisons between the predicted (P), observed (O), and morphologically averaged (MUA) parameters: M4 to M2 amplitude ratio, 2M2-M4 phase lag, and annually averaged flood to tide duration ratio (T_F/T_T) in the chosen year 2013. Gauge locations are given in Fig. 3

Gauge	Unit	A (M2) m	M4/M2 amplitude ratio			2M2-M4 phase lag			T _F /T _T		
			O	P	MUA	O	P	MUA	O	P	MUA
HUI	1	1.05	0.08	0.06	0.07	162	153	153	0.48	0.48	0.49
BOS	2	1.09	0.07	0.05	0.05	170	167	156	0.48	0.49	0.48
KNO	4	1.37	0.13	0.11	0.10	173	164	154	0.49	0.48	0.47
NOY	6	1.15	0.02	0.01	0.03	157	120	110	0.49	0.49	0.48
SPI	8	1.26	0.02	0.02	0.04	140	79	75	0.49	0.50	0.47
WAN	11	1.35	0.05	0.05	0.05	96	80	86	0.47	0.46	0.46
MPL	12	1.43	0.06	0.05	0.06	134	119	113	0.47	0.47	0.47
WAV	14	1.77	0.06	0.05	0.06	190	224	183	0.51	0.52	0.50
ALW	15	1.36	0.05	0.06	0.06	120	104	106	0.47	0.46	0.47
BAL	18	1.74	0.09	0.06	0.07	180	181	167	0.50	0.50	0.49
CUX	22	1.42	0.08	0.09	0.09	114	100	105	0.45	0.45	0.44
BUS	26	1.62	0.04	0.03	0.07	163	160	119	0.49	0.51	0.48
HOH	31	0.97	0.07	0.08	0.08	167	174	157	0.49	0.52	0.49

years represent the diurnal minimum of the nodal tide, which minimizes any astronomical bias. It should be noted that meteorological phenomena and different interannual variations may be present in Fig. 5. However, these processes are unlikely to offset annual averages as, e.g., storm surges are highly episodic and occur only a few times each year. In the following, we use the term *regional* for large-scale processes (e.g., the German Bight) and *local* for processes in the morphological units (e.g., a tidal basin).

A first observation is that flood duration increases by a few minutes in the southwestern German Bight and decreases by up to 20 min in its northeastern part. Regional changes are either enhanced (Southwest) or counteracted (Northeast) within local tidal channels. A second observation is that the regional changes do not carry over into all morphological units. Interestingly, several northeastern tidal channels show increasing flood duration despite a different regional tendency. Similar tendencies are evident in the southeastern German Bight with flood duration increases > 10 min in local tidal channels and slight flood duration decreases in seaward direction. For this reason, we presume that regional tidal dynamics may compete with local processes for flood duration changes.

Inspired by this observation, morphologically averaged trends have been calculated for the flood to tide duration between 1996 and 2016 (Fig. 6). It is notable that morphological units with insignificant linear trends are also displayed, as the consistent temporal evolution of adjacent morphological units may also be of interest (e.g., units 23 to 26). Results yield statistically significant trends in 24 out of 32 morphological units. In accordance with Fig. 5,

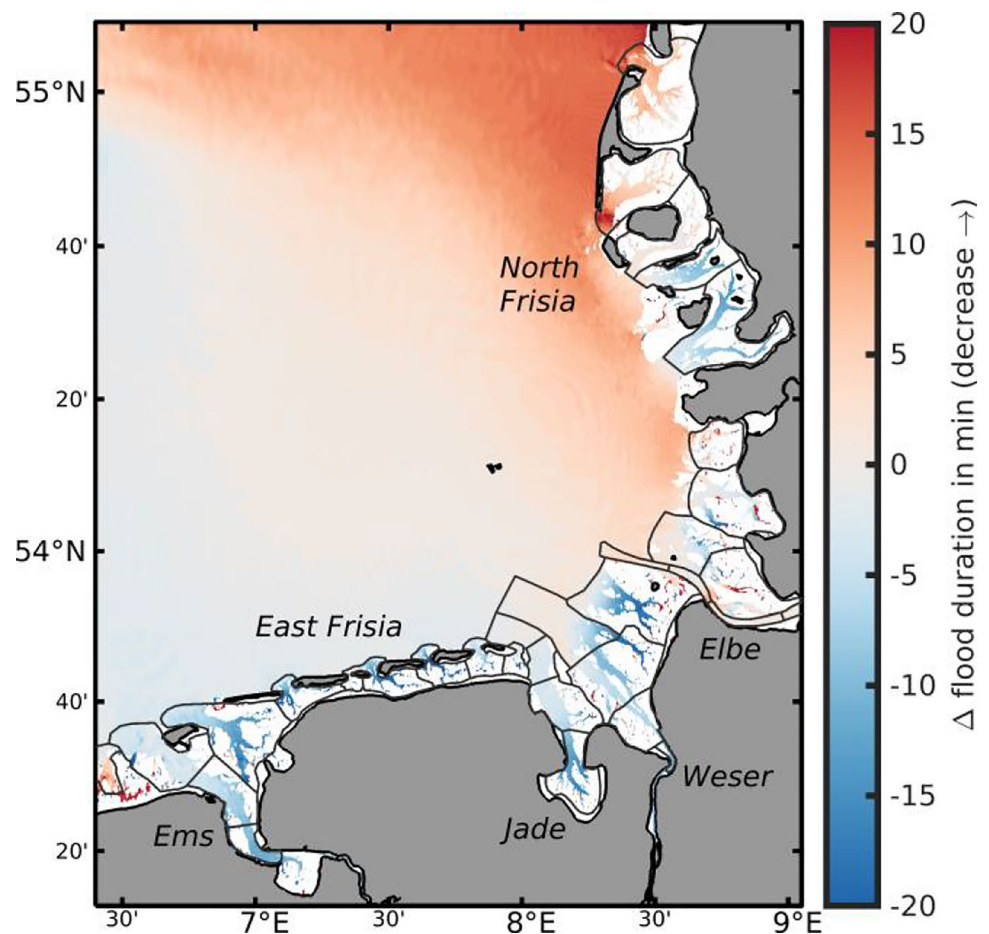
trends reflect a plausible local and regional behavior. The local increase in flood duration (i.e., decreasing flood dominance or increasing flood to tide duration) from units 1 to 18 confirms the findings from Fig. 5. The signal in North Frisia (units 26 to 32) becomes locally both more and less flood dominant; hence, it may be influenced regionally. Specifically, trends in units 27, 31, and 32 show increasing flood dominance, which matches with the evident decrease in flood duration. Conversely, the adjacent units 28 and 30 indicate decreasing flood dominance in accordance with increasing flood durations in Fig. 5.

3.3 Driving factors — changes in tidal range, intertidal storage and subtidal channel volume

In idealized systems, tidal asymmetry can be explained based on morphological constraints such as the tidal amplitude to mean channel depth ratio a/h and the intertidal storage volume V_s to subtidal channel storage V_c ratio V_s/V_c (see Sect. 2.1). We used the EasyGSH-DB bathymetries (Hagen et al. 2021b; Sievers et al. 2021) to estimate a/h and V_s/V_c as defined in Sect. 2.1. In the following, we investigate the development of the tidal range (1), a/h (2), and V_s/V_c (3).

Annual changes in the mean tidal range between 1996 and 2016 in Fig. 7 show regionally varying increases between 3 and 5 mm/a in North Frisia or by less than 2 mm/a in the Ems estuary and in East Frisia. Our increase rates are lower than the recently reported 3.3 mm/a (Jänicke et al. 2020) with a mean increase rate of 1.1 mm/a. We attribute this to slowing increases in the tidal range in the

Fig. 5 Differences between the mean flood duration in 1997 and in 2015 with the blue areas indicating increasing and the red areas indicating decreasing flood duration. The map shows only permanently inundated data in both years. No-data values are represented by white patches, and the morphological units are indicated by black contours



past 20 years (Leon Jänicke, personal communication) compared to the period between 1958 and 2014. Local decreases in units 26 and 27 (near the tidal gauge BUS) have previously been related to local land reclamation and dredging in the Meldorfer Bight (Jänicke et al. 2020). Higher tidal range increase rates in the northeastern German Bight are also in line with current SLR projections (Idier et al. 2017; Wachler et al. 2020; Jordan et al. 2021) and observations (Jänicke et al. 2020). Hence, we can assume locally varying increases in tidal range across the study site with few local exceptions.

Despite the overall increasing tidal range, the alh ratio decreases across the entire study area except for units 1 and 24 to 27, which implies that local subtidal deepening exceeds tidal amplitude increase (in Fig. 8(a)). The largest decreases in alh are found in the river Ems (3, 4) and in the adjacent East Frisian units (5 to 8) as well as the inner Jade (13, 14). The predominant increase in flood duration, e.g., in morphological units 2 to 18 (see Fig. 6), is therefore in line with theoretical expectation that lower alh ratios cause flood dominance to decrease (Friedrichs and Aubrey 1988).

As most alh values from Fig. 8(a) are rather small, the storage-to-channel volume ratio V_s/V_c may determine whether a system is ebb or flood dominant. V_s/V_c in Fig. 8(b) varies between 0 in purely subtidal units in the mouth of the Elbe estuary and 1.8 in East and North Frisia. Most units show an increase in V_s/V_c (3 to 7, 19, and 25 to 32) with unit 27 showing the largest increase. Units 8 to 10 in East Frisia exhibit noteworthy V_s/V_c decreases, which may account for lower increases in flood duration compared to the Ems estuary despite high alh . Figure 8(c) illustrates the relationship between both parameters. For reference, we added the numerical solution of Friedrichs and Aubrey (1988) for flood or ebb dominance. We observe that most points advance further towards the ebb dominant side of Friedrichs and Aubrey's (1988) solution, which is facilitated by the predominant increase in V_s/V_c and the decreasing alh ratios.

However, in contrast to theoretical expectation, Fig. 5 shows that flood duration decreases (i.e., increasing flood dominance) in units 31 and 32 despite a marginal increase in V_s/V_c at constant alh . For this reason, we suggest that changes in tidal amplitude, inter- or subtidal volume are likely counteracted by regional changes in flood duration.

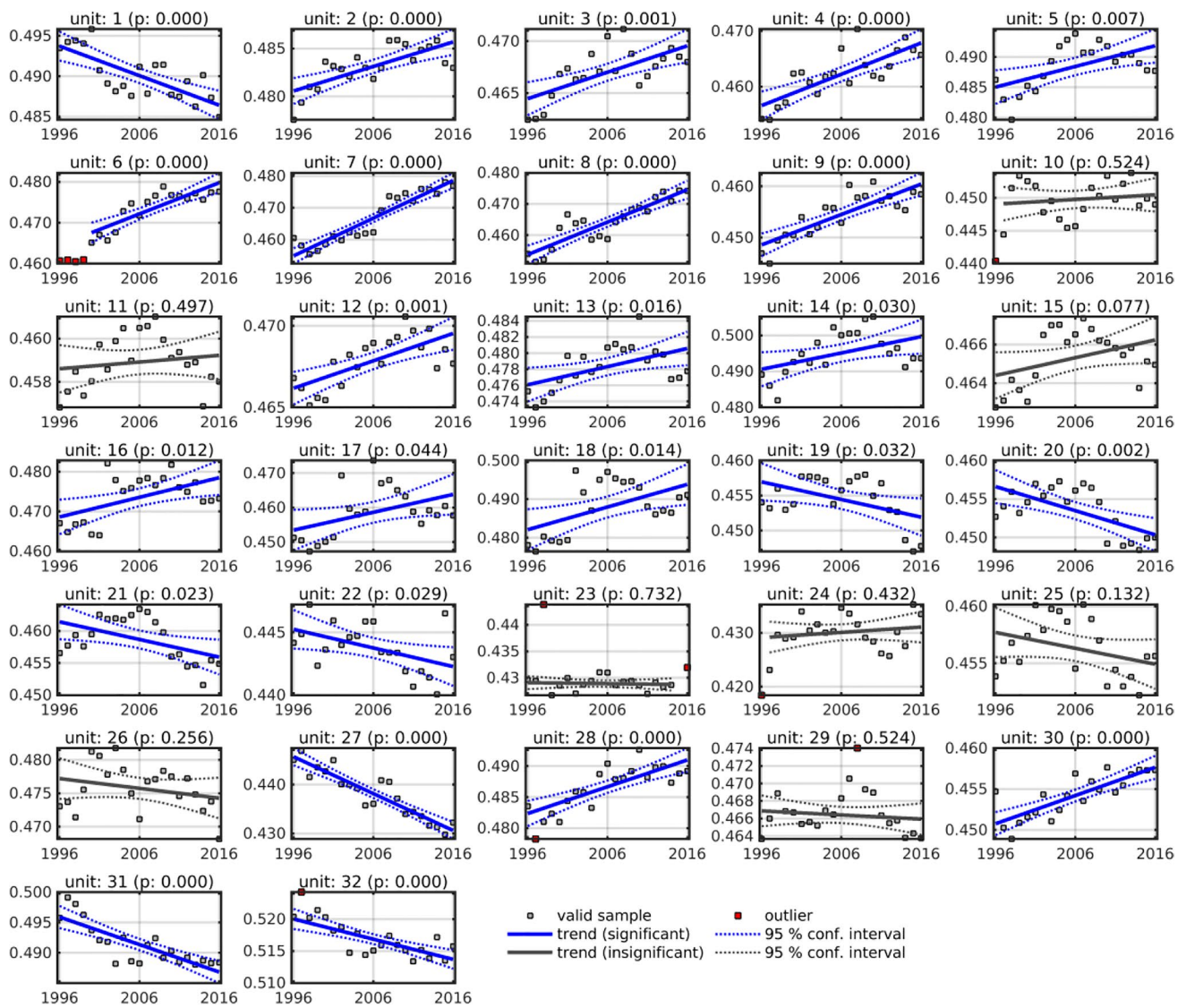


Fig. 6 Linear regression of the flood to tide duration ratio for morphological units from Fig. 3 with ratios <0.5 representing flood dominance. Blue lines indicate significant ($p < 0.05$) trends and their 95% confidence intervals (dashed). Gray lines represent insignificant

fitting with their 95% confidence intervals (dashed). Valid samples within the 95% confidence intervals are represented by gray squares; outliers are represented by red squares. Outliers are not considered in trend estimation and significance testing

Contrary, units 28 to 30 demonstrate increasing flood duration which corresponds well to increasing V_s/V_c .

3.4 Changes in tidal asymmetry

3.4.1 Duration asymmetry

Subsequently, we apply the morphological unit averaging approach (hereafter MUA) to all morphological units between 1996 and 2016 for duration-related tidal asymmetry parameters (see Table 1). The full trend analysis (analogous to Fig. 6) is given in the supplementary material.

We have derived statistically significant trends across the entire study area for the sea surface 2M2-M4 phase lag, the flood to tide ratio, and the flood to tide current duration ratio (see Fig. 9). Results show different regional characteristics mainly with decreasing flood dominance or increasing ebb dominance. The 2M2-M4 phase lag and the flood to tide ratio in Fig. 9(a, b) show decreasing flood dominance in most units in East Frisia and the rivers Ems, Weser, and Jade Bay as well as increasing flood dominance in the river Elbe in unit 27. The 2M2-M4 phase lag, however, indicates an increase in flood dominance in East Frisia, while the flood to tide duration ratio indicates a strong decrease. Trends of adjacent morphological units generally tend to

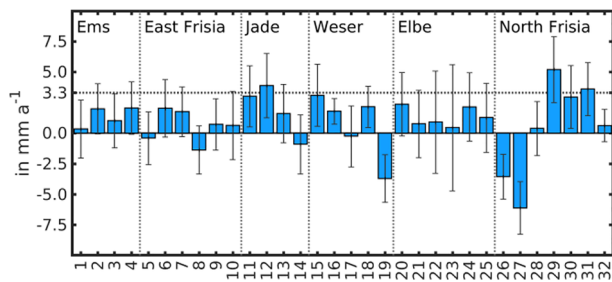


Fig. 7 Morphologically averaged trends of the tidal range with 3.3 mm/a indicating averaged annual tidal range increase at tide gauges from Jänicke et al. (2020). Error bars represent the 95% confidence of the linear regression; blue bars represent the annual trend of the mean tidal range across the morphological units on the x-axis

show a consistent signal within broader regional units, i.e., for East Frisia and the rivers Ems, Weser, and Elbe. North Frisia imposes an exception, as both increasing and decreasing flood dominances are present. This observation is consistent with the spatial differences of flood duration in Fig. 5, which show a similar regional distribution of trends. In addition, we observe local signals such as increasing flood

dominance in the mouth of the Elbe estuary (20 to 25). This local signal is likely related to the development of a second tidal channel in the outer Elbe estuary in the year 2008. The comparison between the 2M2-M4 phase lag and the flood to tide duration is mostly consistent, apart from East Frisia where the 2M2-M4 phase lag indicates increasing flood dominance in some parts. A possible explanation could be the very small M4 amplitudes in most parts of East Frisia (see Table 2).

Flood to tide current duration ratios (Fig. 9(c)) strengthen previous findings about the flood to tide duration ratio (Fig. 9(b)) even though more pronounced changes are evident. We can see either increasing ebb dominance (4, 5, 11 to 13) or decreasing flood dominance (6 to 10) in East Frisia. Units in the Weser and Elbe estuary (15 to 25) demonstrate less variation with few local exceptions. In some cases, trends in sea surface elevation and velocity duration asymmetry do not correspond (e.g., unit 3, 11, or 31).

Unexpectedly, the changes in North Frisia are less pronounced than those in East Frisia, with slight decreases in ebb dominance (26, 27, 29) and decreasing flood dominance

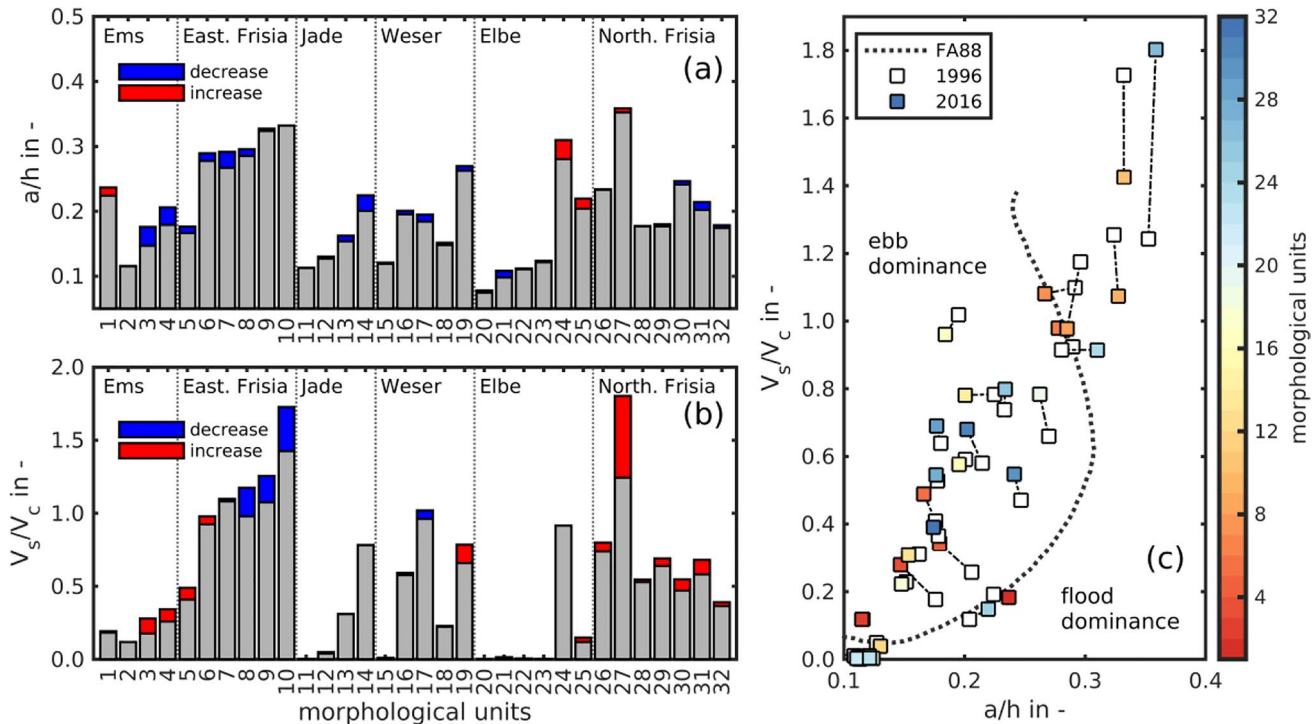
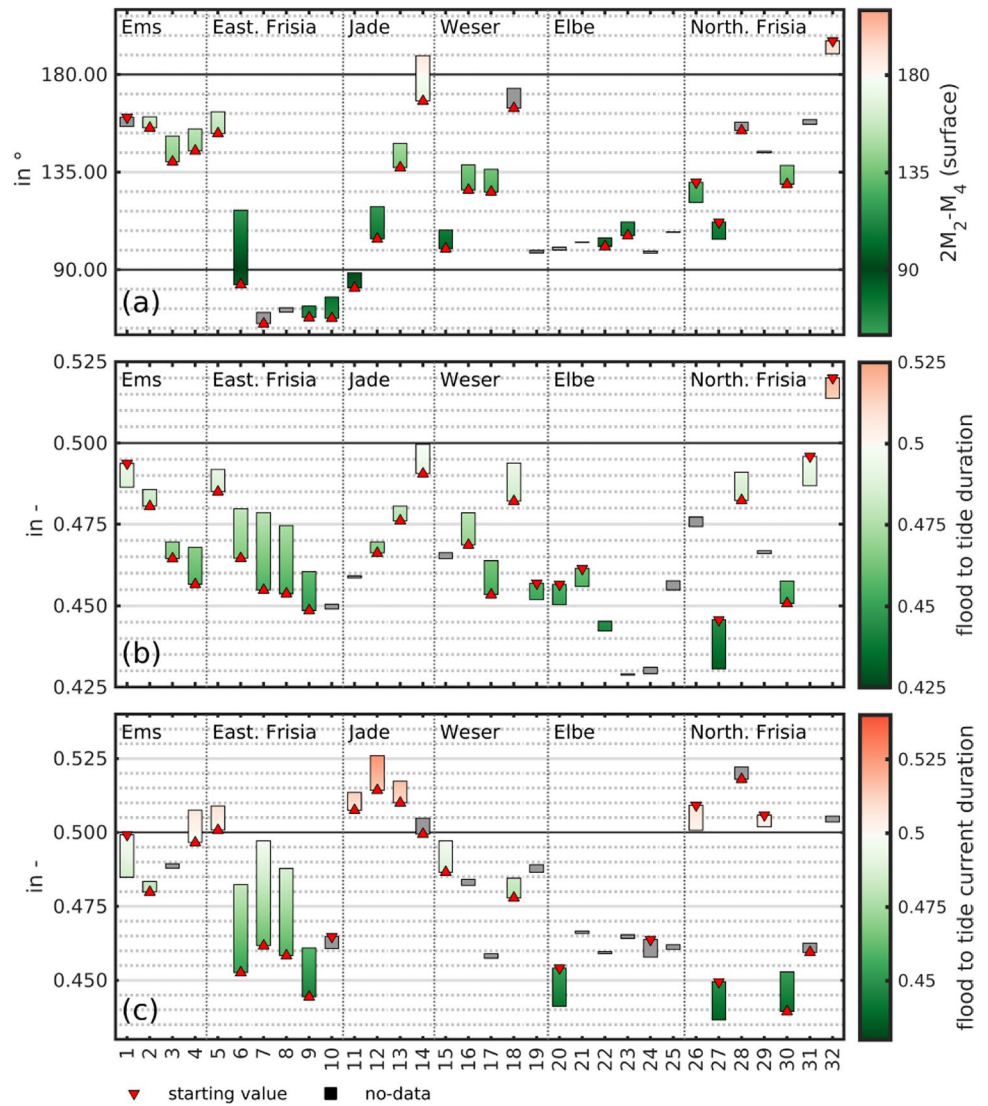


Fig. 8 Changes in the geometrical asymmetry parameters a/h (a), V_s/V_c (b), and a scatterplot of a/h and V_s/V_c (c) with the numerical solution for flood and ebb dominance (dotted gray line) according to Friedrichs and Aubrey (1988). In part (c), the white squares represent the year 1996 which is connected to colored squares in the year

2016. The dot color is determined by the morphological unit index. It should be noted that some of the units are mostly subtidal, which yields very small V_s/V_c ratios. No-data values (e.g., unit 20 in b) can occur if V_s is unavailable due to purely subtidal units. All values are based on linear regression estimates

Fig. 9 Development of the 2M2-M4 phase lag (a), the flood to tide duration ratio (b), and the flood to tide current duration ratio (c) in the period from 1996 to 2016 from linear regression. Gray bars indicate insignificant and colored bars indicate significant trends. The green color represents flood dominance, white represents symmetry, and red represents ebb dominance. Triangles mark the starting point in 1996, and the end of the bar represents 2016. The x-axis represents the morphological units defined in Fig. 3



(30, 31) considering similar changes in tidal amplitude, alh , or V_f/V_e . A comparison of the regional changes (Fig. 5) in duration asymmetry in the context of the morphological development of individual units (Fig. 8) therefore confirms competing local and regional processes. Following Sect. 3.3, we suggest that regionally increasing flood duration (i.e., decreasing flood dominance) in North Frisian tidal channels is partly counteracted by the morphological development, as the tidal amplitude is also dominated by depth changes. However, the local tidal asymmetry trends do not correspond to the morphological asymmetry descriptors, as they are superimposed by regional changes in tidal dynamics. As these trends are absent in the southern German Bight (units 1–18), the morphological development corresponds to the decreasing flood duration.

3.4.2 Current velocity asymmetry

Considering the changes in duration asymmetry and tidal volume, we expect adaptations in the mean flood and ebb current velocity magnitude. For this reason, we evaluated the mean flood and ebb current velocity magnitude with MUA and linear regression in Figs. 10 and 11.

We can see a statistically significant decrease in the mean flood current velocity between units 5 and 19, although the increasing tidal range may suggest otherwise (see Sect. 3.3). The mean flood current velocity decreases by up to 20%, and the mean ebb current velocity increases by approximately 10% in East Frisia. We also observe that across most morphological units, flood current velocity decreases more strongly than ebb current velocity. Hence, Fig. 10 reflects previously demonstrated decreased flood dominance either

by enhanced mean ebb velocity (e.g., 3, 4) or by declining flood velocity (e.g., units 5 to 19). Contrary to the predominantly decreasing velocities, we notice higher flood and ebb current velocity in the Elbe and slightly increased ebb velocity in the Ems estuary, which may be related to local morphodynamics such as the loss of intertidal storage volume or the formation of new tidal channels.

Asymmetric changes in the mean flood and ebb current velocity must provoke a response in current velocity asymmetry, which we have analyzed in Fig. 11. Note that we have scaled ratios < 1 visually to account for the nonlinear behavior of flood to ebb ratios.

We can see in Fig. 11(a) that some morphological units switch from flood to ebb dominance (e.g., 5, 6) or from strong flood dominance to near-symmetry (e.g., 7, 8). We furthermore observe increasing ebb dominance in Jade Bay and the outer Weser estuary (12 to 19). Conversely, the Elbe estuary and North Frisia show both decreasing and increasing flood dominances. Although most units show decreasing flood or increasing ebb dominance, many mean flood to mean ebb current velocity ratios remain flood dominant.

Peak flood to peak ebb current velocity ratios follow the trend of the mean flood to mean ebb current velocity ratio, even though many units are more flood dominant. Small differences between the ratios of mean and peak flood current velocity occur, with different dominances (e.g., 3 and 17) or differing decreases in flood dominance (e.g., 3, 10). Similar to the mean flood to mean ebb current velocity ratio, there is a decreasing flood dominance in East Frisia and increasing ebb dominance in Jade Bay and the Weser estuary. Almost no trends are observed for the mouth of the Elbe, with slightly increasing flood dominance in the inner

units. North Frisian units mostly show declining flood dominance, except for unit 32, which may be attributed to slightly increasing mean ebb velocity at decreasing flood current velocity (see Fig. 10).

4 Discussion

Spatial differences of changes in flood duration between 1997 and 2015 revealed regional and local changes that we investigated in terms of shifts in regional tidal dynamics, increasing tidal range, and local bathymetry evolution. We established a connection between the indication of increasing flood duration in the southern German Bight, a decreased ratio of tidal amplitude to mean water depth a/h , and an increased ratio of subtidal channel to intertidal water volume V_s/V_c . As the tidal amplitude was shown to increase in the German Bight earlier (Jänicke et al. 2020), we suggest that mean subtidal depth increases dominate the development of a/h . For North Frisia, we presumed that the implications of bathymetry changes on tidal asymmetry are partially compensated by shifts in regional tidal dynamics. Methodically, we introduced the morphological unit averaging approach (MUA) to separate local and regional effects in tidal asymmetry by averaging tidal asymmetry parameters in predefined, small subsystems of a larger domain (e.g., a tidal basin) to receive aggregated information for trend analyses. We have applied this approach within the German Wadden Sea for the period of 1996 to 2016 to determine the development of tidal range, tidal asymmetry, and flood and ebb current velocity. We have found decreasing flood dominance or greater ebb dominance for the indicators of duration and current velocity

Fig. 10 Changes in annually averaged mean flood (a) and mean ebb (b) current velocity magnitude in the period from 1996 to 2016 from linear regression with blue increments indicating decreasing and red increments indicating increasing current velocity magnitude. Light gray bars represent insignificant, and dark gray bars represent significant regression

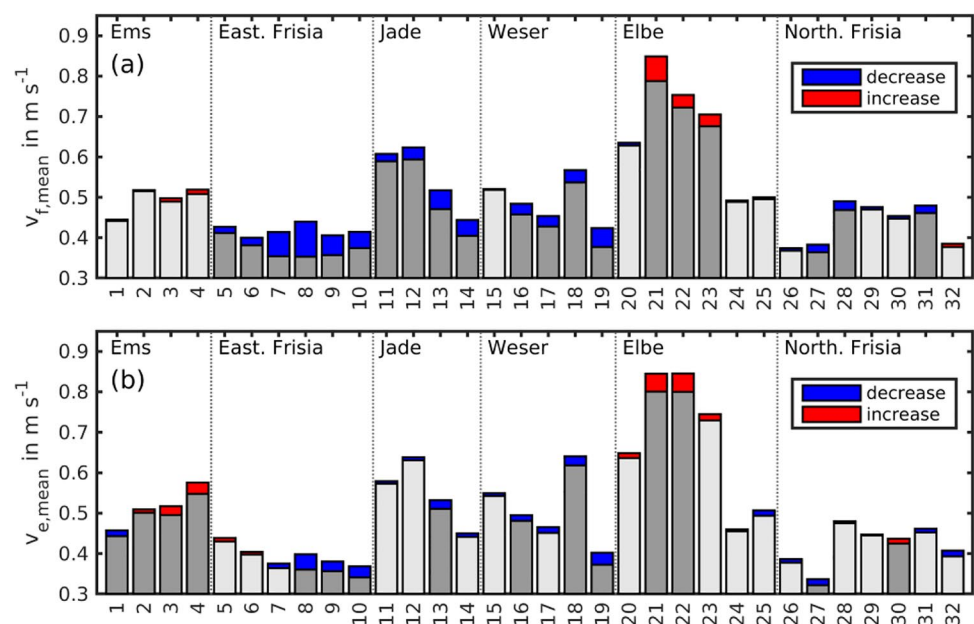
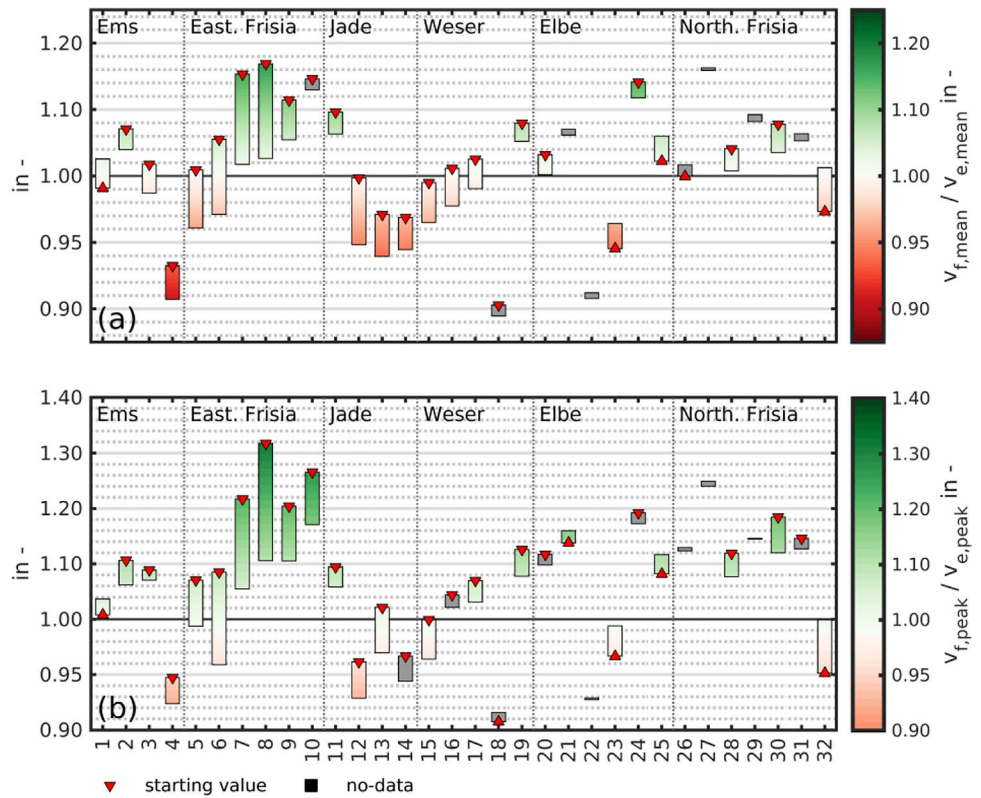


Fig. 11 Trend of the annually averaged mean flood to mean ebb current velocity magnitude ratio (a) and the annually averaged mean peak flood to peak ebb velocity magnitude ratio (b) in the period from 1996 to 2016 from linear regression. Green bars represent flood dominance, white bars represent symmetry, and red bars represent ebb dominance. Triangles mark the starting point in 1996, and the end of the bar represents 2016. The x-axis represents the morphological unit index



asymmetry. The application of morphological averages provides several benefits, such as increased robustness against local processes or the otherwise infeasible description of spatially variable parameters. However, the absence of long-term observational current velocity data in the study area imposes a limitation on our current velocity related results. This problem could be mitigated in the future by increased long-term measuring efforts or additional data from geostationary remote sensing.

Nonetheless, MUA implies several assumptions and simplifications: Multiple averaging steps are needed; i.e., temporal averaging of tidal events to annual tidal characteristic values and spatial averaging within a morphological unit. We proposed an annual averaging of tidal characteristic values because of the variation introduced by interannual changes in tidal asymmetry (Gräwe et al. 2014), seasonally varying run-off, stratification of the pycnocline in shallow coastal seas (Jänicke et al. 2020), and spring-neap dynamics. Additionally, it should be noted that hindcast model data skill in the order of tens of centimeters or minutes, respectively, as well as the inaccuracy of the underlying bathymetry data (Sievers et al. 2021) imposes uncertainty on our results. Still, the agreement of MUA results with measurements (see Table 2) increases our confidence in the presented results. Seasonal time frames, more detailed or coarser morphological unit framing should, however, be the subject of future research.

The comparison of MUA results to tidal gauges has also shown some advantages of the flood to tide duration ratio over the surface 2M2-M4 phase lag in areas with low M4/M2 amplitude ratio. We were able to detect decreasing flood to tide duration ratios in North Frisia, while 2M2-M4 demonstrated no change. It has already been pointed out that the quantification of asymmetry was focused on semi-diurnally dominated systems in the past (Nidzieko 2010) and that other phase relationships may be more appropriate depending on predominate shallow water constituents.

With a few exceptions, all indications in the study area point towards significant decreases in flood dominance or enhanced ebb dominance for sea surface and current velocity. We have shown that most changes are related to the reported increases in mean water depth (Benninghoff and Winter 2019), greater intertidal storage volume, or decreased subtidal channel volume (see Fig. 7). Decreasing flood dominance in the southern German Bight corresponds to decreasing tidal amplitude to mean depth ratio a/h and the decreasing intertidal storage volume V_s to subtidal channel volume V_c ratios (Friedrichs and Aubrey 1988; Friedrichs 2010). These findings are in line with the observed predominant expansion of intertidal flats and the narrowing and deepening of tidal channels (Benninghoff and Winter 2019). Expanding intertidal flats may also play a role in the observed regional changes in tidal dynamics: Intertidal expansion increases net friction, which slows down

the propagation speed of incoming floods, thereby causing longer flood duration. This corresponds to the findings presented by Friedrichs and Madsen (1992), who relate large intertidal width changes in an estuary to ebb dominance. Jordan et al. (2021) showed an increase in energy dissipation of 7% for 0.8 m of sea level rise, with no vertical intertidal flat accretion. This is a reasonable comparison in view of the fact that a larger intertidal area may become available as a result of sea level rise (Guo et al. 2021). The lateral intertidal expansion has also resulted in increased sediment export and greater peak ebb current velocities in a conceptual morphodynamic model of a tidal basin (Guo et al. 2021). Hence, if the intertidal areas expand laterally, the intertidal width changes in the morphological units increase as well, which corresponds to the decreasing flood dominance found in this paper. Stronger decreases in mean flood compared to mean ebb velocity in the study area strengthen the hypothesis of increased friction due to laterally expanding intertidal flats (Guo et al. 2021). Another contributing factor is the decreased subtidal channel volume (Benninghoff and Winter 2019), which likely results in a smaller tidal volume despite increasing tidal range. Recent bathymetry changes as well as increasing V_s/V_c (see Fig. 8(b)) both indicate decreasing channel volume, which supports this hypothesis. It follows that higher frictional resistance on tidal flats and a smaller tidal volume should lead to slower tidal wave propagation across the tidal flats to ultimately lengthen flood duration. Numerical modeling has already shown that a deepening of tidal channels with simultaneous increases in mean tidal flat height leads to a decrease in flood at constant ebb current velocity (Wachler et al. 2020). This agrees with our chain of argumentation.

Morphological units in the mouth of the Elbe estuary and in some North Frisian units, however, show a decreased flood duration (i.e., increasing flood dominance) in contrast to theoretical expectation. Increasing flood dominance in the northern part of North Frisia cannot be explained by shifts of V_s/V_c or alh , which is why we believe other explanations are needed: One possibility is that laterally expanding intertidal flats in the southern German Bight induce additional distortion to the tidal wave through friction before the tidal wave approaches North Frisia (see explanation above). Similar observations were made on the Dutch coast where distorted signals from the English Channel caused flood dominance in adjacent tidal basins of the Dutch Wadden Sea (Dronkers 1986). Another possibility is a shift in the amphidromic system in the German Bight. This hypothesis is supported by recently reported increases in tidal range which were related to shifts of the German Bight amphidromes towards the west (Jänicke et al. 2020). Higher tidal ranges in North Frisia are also visible in our tidal range trend estimation, and they have been shown in sea level rise modeling (Idier et al. 2017; Jordan et al. 2021) and numerical near-coast

bathymetry scenarios (Jacob et al. 2016). Jordan et al. (2021) have explicitly shown a westward drift of the German Bight amphidrome as a response to sea level rise with *and* without vertical intertidal flat accretion. Our results therefore support the hypothesis of regional shifts in the amphidromic system of the German Bight by ruling out bathymetric and tidal amplitude causality in units 31 and 32. Nevertheless, other mechanisms such as stratification changes (Jänicke et al. 2020) or centennial large-scale meteorological and wind cycles (Krieger et al. 2021) may contribute to the trends presented in this paper. However, considerably longer time series would be required to determine these effects.

5 Conclusion and outlook

Previous studies have linked tidal asymmetry of sea surface and current velocity to tidal amplitude, water depth, intertidal storage volume, or subtidal channel volume of a tidal system (Dronkers 1986; Friedrichs and Aubrey 1988; Friedrichs and Madsen 1992). We have analyzed the evolution of concurrent tidal asymmetry and reported bathymetry evolution in the German Wadden Sea (Benninghoff and Winter 2019) in the period from 1996 to 2016. We were able to derive statistically significant trends for spatially variable tidal asymmetry descriptors by applying an average to small subareas (morphological unit averaging approach, MUA) and showed that flood and ebb dominance follow the geometrical considerations reviewed in Friedrichs (2010).

For all domains in the German Bight, declining flood dominance or increasing ebb dominance was revealed with few exceptions only. Our results distinguish between regional shifts in tidal dynamics which compete with local bathymetry evolution. An example is the local decrease in flood duration by more than 10 min in North Frisian tidal basins, despite an increase by more than 15 min in the wider region. Nevertheless, other North Frisian basins showed increased flood dominance, which we related to the earlier reported regional shifts in tidal dynamics of the German Bight (Jänicke et al. 2020; Jordan et al. 2021). Moreover, our results indicate decreasing mean flood and mean ebb velocities in the southern German Bight. This is likely related to increased friction due to laterally expanding intertidal flats (Guo et al. 2021). As all tidal systems worldwide with extensive intertidal storage will be affected by rising sea levels, we expect our results to be applicable for other regions as well. After all, some authors have shown that tidal basins in the German Wadden Sea are resilient to mean sea level rise (Hofstede et al. 2018; Wang et al. 2018) as long as tidal range increases as this promotes sediment accumulation in the intertidal zone (Hofstede 2015). Jänicke et al. (2020) have demonstrated barotropic increases of tidal range in the North Atlantic, which can only be related to meteorological phenomena or sea level rise.

Still, we believe further research is required to quantify the effect of increased intertidal friction and changes in local tidal volume to further solidify our findings.

We would like to emphasize that even though our analysis has shown mostly statistically significant findings, trend quality would improve further if longer time series were available. However, we discourage further extension into the past because bathymetry data before the availability of airborne laser scanning lack accuracy on intertidal flats (Benninghoff and Winter 2019). Future analyses with longer time series may need to refine the linear regression approach as accelerated sea level rise, nonlinear tidal range increase, or limited sediment availability will affect tidal asymmetry in the future.

Decreasing flood dominance will have implications on coastal sediment transport, as decreasing flood dominance may result in reduced sediment import or enhanced sediment export (Guo et al. 2021) in the Wadden Sea. Changes in the duration, mean, and peak current velocity also make changes in sediment composition on intertidal flats and tidal channels likely (Dronkers 1986). If the decline of flood dominance continues, recent sediment accretion on intertidal flats may cease soon. This is a worrying thought, considering the possible drowning of tidal flats due to accelerated sea level rise. It has become clear that further research must be conducted to answer these imminent questions. Even if our findings do not indicate a decline of the Wadden Sea yet, we strongly recommend a continuous annual monitoring program for the Wadden Sea's bathymetry, along with numerical modeling, to be able to track and understand developments and their implications. Furthermore, a corresponding assessment of tidal asymmetry should be extended to the entire trilateral Wadden Sea area and other systems, as it seems reasonable to assume that the trends characterizing these systems are similar to those observed in the German Wadden Sea.

Supplementary Information The online version contains supplementary material available at <https://doi.org/10.1007/s10236-022-01509-9>.

Acknowledgements Robert Hagen would like to express his gratitude to Anna Zorndt for her valuable input at the start of this research and to Anna Wünsche for the constructive and informative discussions about tidal asymmetry.

Author contribution Conceptualization: Robert Hagen, Frank Kösters. Methodology: Robert Hagen, Frank Kösters, Christian Winter. Formal analysis and investigation: Robert Hagen. Plausibility assessment: Christian Winter, Frank Kösters. Writing — original draft preparation: Robert Hagen. Writing — review and editing: Frank Kösters, Christian Winter. Funding acquisition: Frank Kösters. Supervision: Frank Kösters, Christian Winter.

Funding Open Access funding enabled and organized by Projekt DEAL. This paper is part of the research and development project Herkulis which was funded from the research and development program of the Federal Waterways Engineering and Research Institute (Bundesanstalt für Wasserbau, BAW), Germany.

Data availability EasyGSH-DB data collection for bathymetry (Sievers et al. 2020) is available at <https://doi.org/10.48437/02.2020.K2.7000.0002>.

EasyGSH-DB data collection for analyzed tidal dynamics (Hagen et al. 2020) is available at <https://doi.org/10.48437/02.2020.K2.7000.0004>.

Documentation to the EasyGSH-DB data collection is available in Hagen et al. (2021b) and Sievers et al. (2021).

Tide records from Germany must be requested at the local authorities WSV, BfG, and BSH.

Tide records from the Netherlands are available free of charge at <https://waterinfo.rws.nl/>.

We use the EMODnet 2018 DTM WMS web service for visualization (EMODnet 2018).

Code availability Trends were estimated with MATLABs (version: r2020b) *fitlm* function.

Figures were created with QGIS (version 3.16, retrieved October 2020) and MATLAB (version: r2020b).

Harmonic analysis was performed using *UTide* (retrieved June 2020).

Maps were created using the publicly available *m_map* class (retrieved June 2020) and QGIS (version 3.16, retrieved October 2020).

Declarations

Ethics approval Not applicable.

Consent to participate Not applicable.

Consent for publication Not applicable.

Competing interests The authors declare no competing interests.

Open Access This article is licensed under a Creative Commons Attribution 4.0 International License, which permits use, sharing, adaptation, distribution and reproduction in any medium or format, as long as you give appropriate credit to the original author(s) and the source, provide a link to the Creative Commons licence, and indicate if changes were made. The images or other third party material in this article are included in the article's Creative Commons licence, unless indicated otherwise in a credit line to the material. If material is not included in the article's Creative Commons licence and your intended use is not permitted by statutory regulation or exceeds the permitted use, you will need to obtain permission directly from the copyright holder. To view a copy of this licence, visit <http://creativecommons.org/licenses/by/4.0/>.

References

- Becherer J, Hofstede J, Gräwe U, Purkiani K, Schulz E, Burchard H (2018) The Wadden Sea in transition - consequences of sea level rise. *Ocean Dyn* 68:131–151. <https://doi.org/10.1007/s10236-017-1117-5>
- Benninghoff M, Winter C (2019) Recent morphologic evolution of the German Wadden Sea. *Sci Rep* 9:9293. <https://doi.org/10.1038/s41598-019-45683-1>
- Dronkers J (1986) Tidal asymmetry and estuarine morphology. *Neth J Sea Res* 20:117–131. [https://doi.org/10.1016/0077-7579\(86\)90036-0](https://doi.org/10.1016/0077-7579(86)90036-0)
- EMODnet Bathymetry Consortium (2018) EMODnet Digital Bathymetry (DTM 2018), EMODnet Bathymetry Consortium.
- Friedrichs CT (2010) Barotropic tides in channelized estuaries, in: *Contemporary issues in estuarine physics*, edited by: Valle-Levinson,

- A., Cambridge University Press, Cambridge, 27–61, <https://doi.org/10.1017/CBO9780511676567.004>
- Friedrichs CT (2011) Tidal flat morphodynamics, in: *Treatise on estuarine and coastal science*, Elsevier, 137–170, <https://doi.org/10.1016/B978-0-12-374711-2.00307-7>
- Friedrichs CT, Aubrey DG (1988) Non-linear tidal distortion in shallow well-mixed estuaries: a synthesis. *Estuar Coast Shelf Sci* 27:521–545. [https://doi.org/10.1016/0272-7714\(88\)90082-0](https://doi.org/10.1016/0272-7714(88)90082-0)
- Friedrichs CT, Madsen OS (1992) Nonlinear diffusion of the tidal signal in frictionally dominated embayments. *J Geophys Res* 97:5637. <https://doi.org/10.1029/92JC00354>
- Gräwe U, Burchard H, Müller M, Schuttelaars HM (2014) Seasonal variability in M 2 and M 4 tidal constituents and its implications for the coastal residual sediment transport. *Geophys Res Lett* 41:5563–5570. <https://doi.org/10.1002/2014GL060517>
- Guo L, Xu F, van der Wegen M, Townend I, Wang ZB, He Q (2021) Morphodynamic adaptation of a tidal basin to centennial sea-level rise: the importance of lateral expansion. *Cont Shelf Res* 226:104494. <https://doi.org/10.1016/j.csr.2021.104494>
- Hagen R, Plüß A, Jänicke L, Freund J, Jensen J, Kösters F (2021) A combined modeling and measurement approach to assess the nodal tide modulation in the North Sea. *J Geophys Res Oceans*. <https://doi.org/10.1029/2020JC016364>
- Hagen R, Plüß A, Ihde R, Freund J, Dreier N, Nehlsen E, Schrage N, Fröhle P, Kösters F (2021) An integrated marine data collection for the German Bight – part 2: tides, salinity, and waves (1996–2015). *Earth Syst Sci Data* 13:2573–2594. <https://doi.org/10.5194/essd-13-2573-2021>
- Hagen R, Plüß A, Schrage N, Dreier N (2020) EasyGSH-DB: Themengebiet - Hydrodynamik
- Hofstede JLA (2015) Theoretical considerations on how Wadden Sea tidal basins may react to accelerated sea level rise, *zfg*, 59, 377–391, <https://doi.org/10.1127/zfg/2014/0163>
- Hofstede JLA, Becherer J, Burchard H (2018) Are Wadden Sea tidal systems with a higher tidal range more resilient against sea level rise? *J Coast Conserv* 22:71–78. <https://doi.org/10.1007/s11852-016-0469-1>
- Idier D, Paris F, Le Cozannet G, Boulahya F, Dumas F (2017) Sea-level rise impacts on the tides of the European Shelf. *Cont Shelf Res* 137:56–71. <https://doi.org/10.1016/j.csr.2017.01.007>
- Jacob B, Stanev EV, Zhang YJ (2016) Local and remote response of the North Sea dynamics to morphodynamic changes in the Wadden Sea. *Ocean Dyn* 66:671–690. <https://doi.org/10.1007/s10236-016-0949-8>
- Jänicke L, Ebener A, Dangendorf S, Arns A, Schindelegger M, Niehüser S, Haigh ID, Woodworth P, Jensen J (2020) Assessment of tidal range changes in the North Sea from 1958 to 2014. *J Geophys Res Oceans*. <https://doi.org/10.1029/2020JC016456>
- Jordan C, Visscher J, Schlurmann T (2021) Projected responses of tidal dynamics in the North Sea to sea-level rise and morphological changes in the Wadden Sea. *Front Mar Sci* 8:40171. <https://doi.org/10.3389/fmars.2021.685758>
- Krieger D, Krueger O, Feser F, Weisse R, Tinz B, Storch H (2021) German Bight storm activity, 1897–2018. *Int J Climatol* 41:97. <https://doi.org/10.1002/joc.6837>
- Müller M, Cherniawsky JY, Foreman MGG, von Storch J-S (2014) Seasonal variation of the M2 tide. *Ocean Dyn* 64:159–177. <https://doi.org/10.1007/s10236-013-0679-0>
- Nidzieko NJ (2010) Tidal asymmetry in estuaries with mixed semi-diurnal/diurnal tides. *J Geophys Res* 115:185. <https://doi.org/10.1029/2009JC005864>
- Pickering MD, Wells NC, Horsburgh KJ, Green JAM (2012) The impact of future sea-level rise on the European shelf tides. *Cont Shelf Res* 35:1–15. <https://doi.org/10.1016/j.csr.2011.11.011>
- Pickering MD, Horsburgh KJ, Blundell JR, Hirschi JJ-M, Nicholls RJ, Verlaan M, Wells NC (2017) The impact of future sea-level rise on the global tides. *Cont Shelf Res* 142:50–68. <https://doi.org/10.1016/j.csr.2017.02.004>
- Pritchard D, Hogg AJ (2003) Cross-shore sediment transport and the equilibrium morphology of mudflats under tidal currents. *J Geophys Res* 108:1635. <https://doi.org/10.1029/2002JC001570>
- Sievers J, Milbradt P, Ihde R, Valerius J, Hagen R, Plüß A (2021) An integrated marine data collection for the German Bight – part 1: subaqueous geomorphology and surface sedimentology (1996–2016). *Earth Syst Sci Data* 13:4053–4065. <https://doi.org/10.5194/essd-13-4053-2021>
- Sievers J, Rubel M, Milbradt P (2020) EasyGSH-DB: Themengebiet - Geomorphologie
- Song D, Wang XH, Kiss AE, Bao X (2011) The contribution to tidal asymmetry by different combinations of tidal constituents. *J Geophys Res* 116:185. <https://doi.org/10.1029/2011JC007270>
- van Maren DS, Winterwerp JC (2013) The role of flow asymmetry and mud properties on tidal flat sedimentation. *Cont Shelf Res* 60:S71–S84. <https://doi.org/10.1016/j.csr.2012.07.010>
- Wachler B, Seiffert R, Rasquin C, Kösters F (2020) Tidal response to sea level rise and bathymetric changes in the German Wadden Sea. *Ocean Dyn* 70:1033–1052. <https://doi.org/10.1007/s10236-020-01383-3>
- Wang ZB, Elias EPL, van der Spek AJF, Lodder QJ (2018) Sediment budget and morphological development of the Dutch Wadden Sea: impact of accelerated sea-level rise and subsidence until 2100. *Neth J Geosci* 97:183–214. <https://doi.org/10.1017/njg.2018.8>
- Zhou Z, Coco G, van der Wegen M, Gong Z, Zhang C, Townend I (2015) Modeling sorting dynamics of cohesive and non-cohesive sediments on intertidal flats under the effect of tides and wind waves. *Cont Shelf Res* 104:76–91. <https://doi.org/10.1016/j.csr.2015.05.010>